Research Square

Preprints are preliminary reports that have not undergone peer review.
They should not be considered conclusive, used to inform clinical practice,
or referenced by the media as validated information.

Effects of formaldehyde stress on electron transport and reactive oxygen species in moss Racomitrium japonicum L.

Wanting Li
Southwest University of Science and Technology School of Life Sciences and Engineering
Siqi Ma
Southwest University of Science and Technology School of Life Sciences and Engineering
Qunlong Chen
Adminstration Burea of Jiuzhaigou National Nature Reserve
Haiyan Qiu
Southwest University of Science and Technology School of Life Sciences and Engineering
Yunlai Tang
Southwest University of Science and Technology School of Life Sciences and Engineering
Peng Ren
Southwest University of Science and Technology School of Life Sciences and Engineering
Hao Tang
Ecological Pretection and Development Research Institue of Aba Tibetan and Qiang Autonomous Prefecture
Xiaoping Yang
Administration Bureau of Jiuzhaigou National Nature Reserve
Renhua Huang
Jingchu University of Technology
Yunmei Lu
Jingchu University of Technology
Ke Chen
chenke@swust.edu.cn

Southwest University of Science and Technology

Research Article

Keywords: formaldehyde, photosynthesis, reactive oxygen species, antioxidant enzyme system

Posted Date: March 6th, 2024

DOI: https://doi.org/10.21203/rs.3.rs-3851125/v1

License: This work is licensed under a Creative Commons Attribution 4.0 International License.
Read Full License

Abstract

Formaldehyde is a common gaseous pollutant from buildings and decorative materials. However, in recent years, increasing concerns have been raised regarding its harmful health in indoor air. Therefore, this study aims to investigate the physiological and photosynthetic response mechanisms of *Racomitrium japonicum* under formaldehyde stress. *R. japonicum* was exposed to dynamic fumigation with formaldehyde for 7 days, with each day comprising an 8-h exposure period within a sealed container. The effects on plant structure, pigment content, photosynthetic efficiency, and reactive oxygen species (ROS) generation were assessed. Our findings revealed that formaldehyde stress led to structural damage, reduced pigment content, decreased photosynthetic efficiency, and increased ROS production in *R. japonicum*. Significantly, distinct stress-response pathways were observed at various formaldehyde concentrations. In response to low and moderate formaldehyde concentrations, *R. japonicum* activated its antioxidant enzyme system to mitigate ROS accumulation. In contrast, the high-concentration treatment group demonstrated suppressed antioxidant enzyme activity. In response, *R. japonicum* used non-photochemical quenching and activated cyclic electron flow to mitigate severe cellular damage. This study provides an in-depth understanding of the physiological changes of *R. japonicum* under formaldehyde stress, elucidating its response mechanisms. The findings provide valuable information for developing effective indoor formaldehyde monitoring and purification methods.

1. Introduction

Formaldehyde, a common gaseous pollutant emitted from buildings and decorative materials (Adam et al. 2021, Hodgson et al. 2002), can cause irritation to the senses and lead to respiratory illnesses, immune system challenges, and neurological disorders, and even develop causative connections with DNA adducts(Burgos-Barragan et al. 2017, McGregor et al. 2006, Vash 2020). In 2017, the International Agency for Research on Cancer (IARC) of the World Health Organization classified formaldehyde as a Group 1 carcinogen (Anonymous). Given its toxic effects, controlling formaldehyde is of utmost importance. Current techniques for removing formaldehyde from interior environments include physical adsorption, chemical absorption, and catalytic and biological degradation(Peng et al. 2022). Plant-based remediation remains the simplest, most environmentally friendly, and cost-effective alternative among these methods. Early studies by Wolferton et al. suggest that plants could improve indoor air quality by removing organic pollutants(Wolverton 1985). Further research has demonstrated that plant leaves can convert absorbed formaldehyde into carbon dioxide via the Calvin cycle or digest it into amino acids, lipids, free sugars, organic acids, and cell wall components(Kim et al. 2010, Salonen et al. 2009). Besides entering the C1 metabolism through enzymatic reactions, plants can degrade formaldehyde via redox reactions. Liang et al. found that redox interactions between plant oxidants and formaldehyde may constitute the primary mechanism for formaldehyde decomposition in plants. They compared the formaldehyde dissipation capacity of fresh leaf extracts from *Chlorophytum comosum* (Liang et al. 2018). Several common ornamental plants, such as *C. comosum*, *Epipremnum aureum*, *Nephrolepis exaltata*, and some small wild plants, including *Plantago asiatica*, *Taraxacum mongolicum*, and

Cremanthodium delavayi, demonstrated outstanding capabilities in purifying air by absorbing and removing formaldehyde(Xu et al. 2011). Plant remediation is an energy-efficient, ecologically beneficial, and effective method owing to the physiological and metabolic features of plants and their adaptability to the environment. However, comprehensive research on the response mechanisms of plant parameters to formaldehyde exposure is lacking.

Mosses, autotrophic higher plants that transitioned from aquatic to terrestrial habitats, derive their primary nutrients from substrates, rainwater, dew, and deposits generated by atmospheric dust (Bargagli 2016). In recent years, mosses and lichens have gained prominence as monitors and purifiers of pollutants, including heavy metals and radioactive nuclides (Kwon et al. 2021, Mahapatra et al. 2019, Stafilov et al. 2018). Most moss leaves consist of a single or few layers of cells, lack waxy layer, and have large surface area. Some moss species have scales and papillae on their surfaces that provide conditions favorable for the adsorption and retention of air pollutants(Chaligava et al. 2021, Gallego-Cartagena et al. 2021). Moss plants cultivated in harsh environments exhibit signs of damage, such as chlorophyll loss and leaf cell rupture. Changes in atmospheric pollutant composition can also affect its photosynthesis, physiological metabolic pathways, secondary metabolites, and gene stability, leading to changes in biological traits and physiological-biochemical parameters (Bargagli 2016, Krommer et al. 2007).

Mosses possess distinctive physiological adaptation mechanisms that enable them to survive in environments that pose challenges, such as high temperatures, extremely cold conditions, and drought, compared to other terrestrial plants. This makes them ideal for monitoring and validating atmospheric pollution (Sheng et al. 2022, Świsłowski et al. 2021). Owing to their ornamental and economic value, moss plants are well-suited for short-term artificial cultivation and propagation. They offer easy management and a cost-effective approach to monitoring. Therefore, this study aims to investigate the photosynthetic and antioxidant physiological responses of *R. japonicum* under formaldehyde stress. This study can potentially provide valuable insights into the monitoring of indoor toxic gases.

2. Material and methods

2.1 Plant materials and treatments

The moss (*R. japonicum*) utilized in this study was collected from Hanzhong, Shanxi. The moss samples were cultivated in a controlled greenhouse environment after thoroughly rinsing with deionized water to eliminate pebbles and weeds. The cultivation conditions included a diurnal temperature cycle of 25/20°C, light intensity of 2000 lx, and relative humidity ranging from 60–70%. The moss samples were categorized into four distinct groups: control, low-concentration (10 mg/m^3), moderate-concentration (50 mg/m^3), and high-concentration (100 mg/m^3). Following a 7-day cultivation period, *R. japonicum* was carefully transferred to glass culture dishes with a diameter of 11 cm. These dishes were then placed inside a hermetically sealed fumigation chamber measuring 40 cm in length, width, and height, respectively. After closing the chamber, different volumes of formaldehyde were introduced, and the

samples were subjected to an 8-h treatment each day, spanning from 9:00–17:00, for 7 days. After the treatment, samples were collected to measure various photosynthetic and physiological parameters.

2.2 Morphological and structural analysis

Two to three roots of *R. japonicum*, treated for 7 days, were selected for photography. An appropriate amount of *R. japonicum* was taken, washed, and dried at 70°C until a constant weight was achieved, ground into powder using liquid nitrogen, and then subjected to microstructure photography using a scanning electron microscope (SEM).

2.3 Determination of chlorophyll content

In this study, *R. japonicum* was prepared by weighing 0.3 g of the plant material, which was then finely chopped and placed into a 10 mL stoppered test tube. To facilitate extraction, 10 mL of a specific extraction solution consisting of a mixture of acetone and ethanol at a 1:1 ratio (v/v) was added to the test tube. The tube was securely covered and stored in a light-protected environment at 25°C for 24 h to allow for optimal extraction. After the moss plant leaves had completely discolored, indicating successful extraction, the contents of the test tubes were thoroughly mixed by shaking. Subsequently, a volume of 200 µL was withdrawn from the test tube to measure the absorbance of the extracted solution at two specific distinct wavelengths, 663 and 645 nm. This absorbance measurement served as a quantitative indicator of the desired compounds in the extraction solution.

2.4 Fluorescence imaging

Chlorophyll fluorescence imaging and related parameters of *R. japonicum* were measured using MINI-Pam (red LED version) and the imaging fluorometer software Win (Heinz Walz, Germany). Before measurement, the leaves were subjected to a 30 min dark treatment. The measurement light frequency was set to 1 Hz, intensity to 1 µmol/m^{-s}, photochemical intensity to 101 µmol/m^{-s}, saturation pulse intensity to 2800 µmol/m^{-s}, the duration to 30 s, and imaging area to 24 mm × 32 mm (Li et al. 2023).

2.5 Determination of fast chlorophyll fluorescence-induced kinetic curves

Chlorophyll fluorescence induction kinetics was rapidly assessed using a plant efficiency analyzer (M-PEA, Hansatech). When leaves were exposed to high-density photochemical light (10,000 µmol photons $m^{-2}s^{-1}$), the fluorescence transient indicated a multiphase rise in O-, J-, I-, and P-phases. This multiphase rise in fluorescence transients reveals information regarding photosystem II (PSII) photochemistry, including electron transfer between the donor and acceptor sides of PSII. The four characteristic points on the OJIP curves (O, J, I, and P) correspond to time points of 0, 2, 30, and 1000 ms, respectively, with relative fluorescence intensities denoted by F_O, F_J, F_I, and F_P, respectively. The time points corresponding to 0.15 and 0.3 ms on the OJIP curve are designated as the L and K characteristic points, with corresponding relative fluorescence intensities denoted by F_L and F_K, respectively(Tang et al. 2020). The OJIP curves for various treatments were normalized using O-P, O-J, and O-K–K. Normalization involved

setting the relative fluorescence intensity at point O as 0 and at points P, J, and K as 1. The normalization equations used were V_{O-P} = (Ft-Fo)/(Fp-Fo), V_{O-J} = (Ft-Fo)/(FJ-Fo), and V_{O-K} = (F_t-F_o)/(F_k-F_o). where F_t represents the relative fluorescence intensity at different time points. The relative variable fluorescence intensities of the four characteristic points L, K, J, and I on the standardized curves are expressed as V_L, V_K, V_J, and V_I, respectively. Before fluorescence measurements, all samples underwent a 30-min dark adaptation.

2.6 Rapid light response curve determination

The measurement system used for simultaneous PSI and PSII measurements was the Dual-PAM 100 (Heinz Walz). To deplete the photosynthetic electron pool, plants were subjected to a 60-min dark adaptation. Subsequently, light at 500-μmol photons m^{-2} s^{-1} was applied for 5 min to activate the photosynthetic electron pool. The plants were then exposed to gradually increasing light intensities (0–1181 mol photons m^{-2} s^{-1}) to establish the light response curves.

For PSI, the following parameters were calculated: Y(I) = (Pm'-P)/Pm; Y(ND) = P/Pm; Y(NA) = (Pm-Pm')/Pm, where Y(I) represents the photochemical quantum yield of PSI, Y(ND) represents the proportion of oxidation state of PSI reaction center P700, and Y(NA) represents the proportion of the reduced state of PSI reaction center P700.

The PSII parameters were calculated as follows: Y(II)=(Fm'/Fs)/Fm'; non-photochemical quenching (NPQ)=(Fm-Fm')/Fm'; Y(NO) = Fs/Fm. where Fm represents the maximum chlorophyll fluorescence intensity after dark adaptation. Fm' denotes the maximum chlorophyll fluorescence intensity after light adaptation. Fs are the steady-state fluorescence intensity following light acclimation. Y (II) denotes the effective photochemical quantum yield of PSII, NPQ is the non-photochemical quenching capacity of PSII, and Y (NO) denotes the non-regulatory heat dissipation of PSII.

The photosynthetic electron transfer rate was calculated using the following equation: ETRI = PPFD × Y (I) × 0. 84 × 0. 5; ETRII = PPFD × Y (II) × 0.84 × 0. 5. where ETRI and ETRII represent the electron transfer rates through PSI and PSII, respectively; ETRI-ETRII represents the cyclic electron transfer (CEF) rates; and PPFD represents the photosynthetic effective radiation intensity (Xia et al. 2022).

2.7 Determination of reactive oxygen content and staining localization

To determine hydrogen peroxide content, 0.1 g of the plant was taken and homogenized in liquid nitrogen with the addition of 1.7 mL of 0.1% TCA. The resulting homogenate was then centrifuged at 4°C for 15 min at 12,000 r/min. Subsequently, 1 mL of the supernatant was mixed with 0.2 mL of 1M KI and 0.1 mL of 0.1M potassium phosphate buffer (pH 7.0). This mixture was left to react in darkness at room temperature for 1 h. The absorbance at 390 was measured using 0.1% TCA as a reference. The absorbance at 390 was measured using 0.1% TCA as a reference(Yesbergenova et al. 2005).

To determine superoxide anion content, 0.1 g of the plant was weighed and homogenized with 0.4 mL of 0.5 M potassium phosphate buffer (pH 7.4). The resulting homogenate was extracted for 10 min at 4 ℃ and 3500 r/min. Following this, 0.5 ml of the extract was mixed with 0.5 mL of 0.05 M potassium phosphate buffer (pH 7.8), and 1 mL of 1 mM hydroxylamine hydrochloride was added. The mixture was shaken well and then incubated at 25℃ for 1 h. Subsequently, 1 mL of 17 mM p-aminobenzene sulfonic acid and 1 mL of 7 mM α-naphthylamine were added sequentially, mixed with rapid shaking, and incubated for an additional 1 h at 25℃. The mixture was quickly mixed and shaken well after adding 1 mL of 17 mM p-aminobenzenesulfonic acid and 1 mL of 7 mM α-naphthylamine (Yergaliyev et al. 2016). Subsequently, the samples were kept at 25°C for 20 min, followed by centrifugation at 3000 r/min for 3 min. The pink aqueous phase was then measured at 530 nm and zeroed with distilled water. The rate of superoxide anion production was determined from the NO_2^-standard curve and fresh weight (FW).

To determine malondialdehyde (MDA) content, 0.2 g of the plant was weighed and extracted in two batches using a 10% TCA solution, bringing the final volume to 2 mL. The extraction was centrifuged at 3000 r/min for 10 min, and the resulting supernatant was retained for measurement. In the color reaction step, 1 mL of the supernatant and 2 mL of a 0.6% thiobarbituric acid solution were combined in a stoppered test tube. The mixture was well-mixed, covered, and placed in a boiling water bath for 20 min to develop the color. After rapid cooling, the solution was centrifuged. (Srivastava et al. 2017). The absorbance values at 532, 600, and 450 nm were then determined for the supernatants.

Hydrogen peroxide-positioned staining-diaminobenzidine method: 50 mL of 1 mg/mL 3,3-diaminobenzidine (DAB) solution was adjusted to a pH of 3.0 with 0.2 M HCl. To this solution, 25 µL of Tween-20 (0.05% V) and 2.5 mL of 200 mM Na_2HPO_4 were added. Owing to the light-sensitive nature of the DAB, precautions were taken to shield it from light (Achary et al. 2008). The moss plants subjected to treatment were fully immersed in the DAB staining solution and placed in a shaker at 80–100 rpm, 25°C, for 4 h, during which they were shielded with tin foil. After staining, the plants were bleached using a bleach solution [anhydrous ethanol (V): acetone (V) = 1:1] in a boiling water bath for 15 min.

Superoxide anion staining-nitrotetrazolium chloride blue method: 0.05 g of nitrotetrazolium chloride blue (nitroblue tetrazolium [NBT]) was weighed and dissolved in 50 mM phosphate buffer (pH 7.5) to obtain 50 mL of NBT-stained solution with a concentration of 0.1%(Rao &Davis 1999). The moss plants were immersed in the staining solution and stained in the dark for 12 h at 25°C. The color was then removed in two steps using a bleaching solution [acetone (V) + anhydrous ethanol (V) = 1:1 and anhydrous ethanol (V): glacial acetic acid (V): glycerol (V) = 3:1:1].

2.8 Determination of antioxidant enzyme system activity

Superoxide dismutase (SOD), peroxidase (POD), and catalase (CAT) levels were measured using kits manufactured by the Nanjing Jianjian Bioengineering Institute, while ascorbate peroxidase (APX), dehydroascorbate reductase (DHAR), and monodehydroascorbate reductase (MDHAR) levels were measured using kits manufactured by Solepol.

2.9 Statistical analysis

Data were presented as the means ± SE of independent measurements. Group differences were evaluated using one-way analysis of variance (ANOVA), followed by Duncan's new multiple range test at a significance level of $p < 0.05$, using SPSS 18.0. Basic visualization and data processing were performed using Origin 2018 software.

3. Results

3.1 Morphological and structural effects of formaldehyde stress on *R. japonicum*

Formaldehyde fumigation partially disrupted the morphology of *R. japonicum*. The influence of formaldehyde stress caused the green color of *R. japonicum* leaves to transition to yellow. The degree of yellowing was positively correlated with formaldehyde concentration (Fig. 1A). Initially, at low concentrations, yellowing was observed exclusively at the leaf tips; however, as the concentration increased, yellowing gradually spread downwards along the leaves. All parts of *R. japonicum* in the high-concentration group had yellow hues. To understand the changes in the *R. japonicum* microstructure, we used an SEM. In the control group, the moss exhibited a well-organized surface structure with uniform interstices. In contrast, the moss in the low-concentration group showed a gradual thinning of the surface structure. As formaldehyde concentration increased in the medium- and high-concentration groups, the disruption of the moss surface structure increased, leading to larger gaps and a more dispersed distribution (Fig. 1C).

3.2 Effect of formaldehyde stress on chlorophyll content and fluorescence imaging of the *R. japonicum*

When plants are exposed to external environmental stress, the chlorophyll content serves as an effective indicator of photosynthetic damage. The low-concentration group exhibited a reduction of 19.7% in chlorophyll a content and a 23.4% decrease in chlorophyll b content compared to the control group. Similarly, the moderate concentration group displayed a significant decline of 55.9% in chlorophyll a content and a 35.1% decrease in chlorophyll b content. Significantly, the high-concentration group experienced a substantial decrease of 68.9% in chlorophyll a content and a reduction of 54.2% in chlorophyll b content (Table 1). These findings highlight the heightened sensitivity of *R. japonicum* chlorophyll content to formaldehyde exposure. Furthermore, in the moderate and high concentration groups, the chlorophyll a/b ratios were decreased by 31.3% and 32.1%, respectively, compared to the control group. In contrast, the low-concentration group showed no significant changes.

Chlorophyll fluorescence imaging of *R. japonicum* (Fig. 2) and chlorophyll fluorescence parameters (Table 2) provided valuable insights into the effects of formaldehyde stress on photosynthesis. Fv/Fm, a commonly utilized and frequently measured parameter in chlorophyll fluorescence analysis, serves as an

indicator of the maximum photosynthetic efficiency of photosystem II, reflecting the ability of the plant for optimal light energy conversion. After exposure to varying formaldehyde concentrations, the Fv/Fm values of *R. japonicum* decreased significantly. Specifically, the low, moderate, and high-concentration groups exhibited an 11.4%, 21%, and 27.4% decrease, respectively, compared to the control group. Y(II), representing the actual photosynthetic efficiency of photosystem II, accurately represents the current light-energy conversion efficiency of the photosynthetic apparatus. Under formaldehyde stress, Y(II) in *R. japonicum* significantly declined with increasing formaldehyde concentrations ($P < 0.05$). Fluorescence quenching can occur due to enhanced photosynthetic activity or increased thermal dissipation during photosynthesis. Photochemical quenching (qP) refers to fluorescence quenching resulting from photosynthesis. In contrast, non-photochemical quenching (qN) describes fluorescence quenching arising from thermal dissipation. Compared to the control group, qP decreased by 11%, 32.3%, and 42.9% in the low, moderate, and high concentration groups, respectively, indicating a decrease in photosynthetic activity under formaldehyde stress. Moreover, compared with the low-concentration group, qN increased by 20% and 38.4% in the moderate and high-concentration groups, respectively.

Table 1
Chlorophyll content of *Racomitrium japonicum* after formaldehyde stress

	Chla(μg·mg^{-1})	Chlb(μg·mg^{-1})	Chla/Chlb
CK	0.177 ± 0.001^{a}	0.094 ± 0.001^{a}	1.877 ± 0.024^{a}
LOW	0.142 ± 0.003^{b}	0.072 ± 0.002^{b}	1.983 ± 0.001^{a}
MODERATE	0.078 ± 0.003^{c}	0.060 ± 0.002^{c}	1.289 ± 0.086^{b}
HIGH	0.055 ± 0.001^{d}	0.043 ± 0.002^{d}	1.274 ± 0.067^{b}

Values are expressed as means ± SE (n = 3). Different letters represent significant differences between the treatments ($p < 0.05$).

3.3 Fast-phase fluorescence of chlorophyll

To better understand the changes occurring in photosystem II of *R. japonicum* under formaldehyde-induced stress, we analyzed the rapid chlorophyll fluorescence induction kinetics curve, commonly referred to as the OJIP curve (Fig. 3A). The O point on the curve indicates the initial fluorescence. In contrast, the P point represents the peak fluorescence intensity. Following exposure to formaldehyde, the O and P points decreased their values, corresponding to increasing formaldehyde concentrations. To standardize the OJIP curve, it was normalized to the Fm-Fo baseline. Subsequently, Vt was calculated by subtracting the kinetics of the treated group from those of the control group (Fig. 3B). Comparative analysis revealed distinct variations in the formaldehyde-treated samples compared with the control group. Specifically, the appearance of L and K peaks was observed, with the L peak attaining its highest magnitude in the high-concentration group (Fig. 3C, D).

3.4 Effect of formaldehyde stress on the rapid light response curve of *R. japonicum*

The rapid light-response curve provides real-time insights into the physiological status of photosynthesis. Y(I) represents the actual photochemical efficiency of photosystem I (PSI). The PSI photochemical quantum yield Y(I) decreased with increasing light intensity (Fig. 4A). Starting from an illumination intensity of 135-μmol photons $m^{-2}s^{-1}$, the middle and high concentration groups show significantly lower Y(I) values than the control group. This indicates a reduction in the actual photochemical efficiency of PSI in *R. japonicum* under moderate to high formaldehyde stress, leading to the functional impairment of PSI. Y(ND) represents the quantum yield of nonphotochemical dissipation caused by the donor-side limitation of PSI (Fig. 4B). From an illumination intensity of 135-μmol photons $m^{-2}s^{-1}$, the Y(ND) values in the middle and high concentration groups are significantly higher than those in the control group, suggesting an elevation in donor-side limitation of PSI under moderate to high formaldehyde stress. Y(NA) represents the quantum yield of non-photochemical dissipation caused by acceptor-side limitation in PSI. The values in all groups were relatively low and showed no significant changes. Y(II) represents the actual photochemical efficiency of photosystem II (PSII). The middle and high concentration groups showed significantly lower Y(II) values than the control group, suggesting that moderate to high formaldehyde stress restricts the functionality of PSII (Fig. 4D). Y(NO) represents the quantum yield of non-regulated energy dissipation in PSII and serves as an indicator of photodamage. The Y(NO) values in the intermediate and high formaldehyde concentration groups were significantly higher than those in the control group. This suggests that moderate-to-high formaldehyde stress caused a certain degree of photodamage to the photosynthetic apparatus (Fig. 4E). Y(NPQ) represents the energy absorbed by PSII, dissipating as heat and serving as a photoprotection indicator (Fig. 4F). At an illumination intensity of 135–275 μmol photons $m^{-2}s^{-1}$, the high concentration group demonstrated significantly higher Y(NPQ) values compared to the other treatment groups, suggesting the activation of thermal dissipation as a protective response to formaldehyde stress under low light conditions. However, at an illumination intensity of 1181-μmol photons $m^{-2}s^{-1}$, the high-concentration group showed significantly lower Y(NPQ) values than the control and low-concentration groups. This decrease could be attributed to high light intensity, potentially limiting the thermal dissipation mechanism in *R. japonicum.*

ETRI represents the relative linear electron flow through Photosystem I, whereas ETRII denotes the relative linear electron flow through Photosystem II. The middle- and high-concentration groups demonstrated significantly lower ETRI and ETRII values than the control group (Fig. 4G and H), suggesting that formaldehyde stress concurrently affected the photosynthetic efficiency of both PSII and PSI. The difference between ETRI and ETRII is known as CEF. At an illumination intensity of 135–424 μmol photons $m^{-2}s^{-1}$, the high-concentration group showed significantly higher CEF values than the control and low-concentration groups, indicating CEF activation in response to high formaldehyde concentration to alleviate photodamage to PSI (Fig. 4I). A rectangular hyperbolic model was used for nonlinear fitting to quantitatively describe the rapid light-response curve. The fitted parameters (Table 2) included α, representing the initial slope of the rapid light response curve, reflecting the efficiency of the

photosynthetic organ in utilizing light energy. Under the high formaldehyde concentration treatment, the initial slope of the rapid light response curve in *R. japonicum* significantly decreased, indicating a significant reduction in the efficiency of light energy utilization by the photosynthetic organs. ETRmax represents the potential maximum relative electron transport rate derived from the fitting. The ETRIImax values in the low-, middle-, and high-concentration groups were significantly lower than those in the control group. This suggests that formaldehyde stress affects electron transport in *R. japonicum*, with PSII being the most susceptible to formaldehyde. Additionally, the ETRIImax values in the low- and middle-concentration groups were significantly lower than those in the control group, indicating impairment of the electron transport capacity in PSI caused by moderate to low formaldehyde concentrations. Nevertheless, no significant difference was observed between the high-concentration and control groups. Point Ik, representing the intersection of the initial slope line with the ETRmax level on the x-axis, reflects the tolerance of the sample to high light intensity. No significant difference was observed in PSII between the high-concentration and other treatment groups. In contrast, in PSI, the high concentration group showed a significant increase than the low and medium concentration groups. This increase may be because of the activation of cyclic electron flow around PSI, thereby enhancing the tolerance of the plant to high light intensity.

Table 2
Parameters for *R. japonicum* light response curve fitting under different concentrations of formaldehyde stress

	Parameters of RLCs of ETR(I)			**Parameters of RLCs of ETR(II)**		
	α (e^- Photon^{-1})	ETRmax (μmol e^- m^{-2} s^{-1})	Ik (μmol Photon m^{-2} s^{-1})	*α* (e^- Photon^{-1})	ETRmax (μmol e^- m^{-2} s^{-1})	Ik (μmol Photon m^{-2} s^{-1})
CK	0.468 ± 0.020^{a}	169.060 ± 17.865^{a}	360.897 ± 49.196^{ab}	0.509 ± 0.038^{a}	94.586 ± 12.756^{a}	185.747 ± 35.171^{a}
LOW	0.476 ± 0.024^{a}	117.235 ± 6.271^{b}	246.240 ± 20.551^{b}	0.574 ± 0.078^{a}	64.010 ± 2.895^{b}	111.489 ± 29.975^{ab}
MODERATE	0.462 ± 0.028^{a}	101.664 ± 7.627^{b}	219.854 ± 28.491^{b}	0.680 ± 0.119^{a}	37.148 ± 3.180^{c}	54.596 ± 9.827^{b}
HIGH	0.292 ± 0.035^{b}	129.340 ± 18.447^{ab}	442.499 ± 93.426^{a}	0.223 ± 0.054^{b}	21.973 ± 5.897^{c}	98.489 ± 23.746^{ab}

Values are expressed as means ± SE (n = 3). Different letters represent significant differences between the treatments ($p < 0.05$).

3.5 Changes in antioxidant physiology of *R. japonicum* under formaldehyde stress

To analyze the effect of formaldehyde stress on oxidative damage to the photosystems of *R. japonicum*, we measured the accumulation of reactive oxygen species (ROS). The treatment groups demonstrated elevated levels of superoxide anion ($O_2^{\cdot-}$), hydrogen peroxide (H_2O_2), and MDA compared to the control group (Fig. 5A, B; Fig. 6). Specifically, the low concentration group showed a 24.1% increase in $O_2^{\cdot-}$ accumulation than that in the control group. Additionally, the MDA content in the medium-concentration group was 6.6 times higher than that in the control group. The accumulation of ROS in *R. japonicum* was most pronounced under high formaldehyde stress, exhibiting 2.1, 1.36, and 11.7 times higher levels of $O_2^{\cdot-}$, H_2O_2, and MDA, respectively, compared to the control group. Tissue staining with NBT for superoxide anions revealed purple staining in the *R. japonicum* leaves after formaldehyde treatment (Fig. 5A), with the highest intensity and distribution observed in the high-concentration group. Additionally, tissue staining using DAB for hydrogen peroxide showed brown deposits at the tips of *R. japonicum* leaves under formaldehyde treatment (Fig. 5B), with both intensity and the number of staining sites increasing with higher formaldehyde concentrations. These findings indicate that the accumulation of ROS in *R. japonicum* gradually rises with increasing formaldehyde concentrations, indicating that the presence of formaldehyde can induce oxidative damage in the plant.

Following oxidative damage, plants activate various protective mechanisms, with the antioxidant enzyme system being the key mechanism for ROS clearance. Under low-concentration formaldehyde stress, the activities of SOD, POD, and CAT increased significantly (Fig. 7A–C). Under moderate formaldehyde treatment, SOD and POD activities significantly increased. In contrast, CAT showed no significant difference compared with the control group. However, under high formaldehyde stress, the activities of SOD, POD, and CAT decreased significantly ($P < 0.05$). This indicates that the antioxidant enzyme system can effectively function within a certain range of formaldehyde concentrations to clear ROS. However, its activity decreases under high concentrations of formaldehyde. Apart from the antioxidant enzyme system, non-enzymatic antioxidants also play a role in ROS clearance. In the ascorbate-glutathione cycle, the activities of MDHAR and DHAR in the low-concentration group were reduced by 54.2% and 8.42%, respectively, compared to the control group. In the moderate concentration group, MDHAR and DHAR activities were reduced by 80.2% and 26.9%, respectively, compared to the control group. In the high-concentration group, the activities of APX and MDHAR were reduced by 61.3% and 67.1%, respectively, compared to the control group (Fig. 7D–F).

4. Discussion

4.1 Effects of formaldehyde stress on the morphological structure of *R. japonicum*

Scanning electron microscopy revealed the emergence of protrusions on the surface of *R. japonicum* (Fig. 1B), enhancing the surface contact area of the leaves and promoting the adsorption of substances from the air. The morphology of the plant is highly indicative of the air quality in its surrounding environment. After exposure to moderate and high formaldehyde concentrations, *R. japonicum* leaves

displayed wilting and a color change from green to yellow. Scanning electron microscopy revealed a transition in *R. japonicum* microstructure from a dense and orderly arrangement to a disordered state. Previous studies have shown that 15 hydroponic plants exhibited varying forms of morphological damage, such as leaf surface damage, tip withering, and leaf wilting, after exposure to different concentrations of formaldehyde fumigation. The degree of damage can serve as an indicator of plant resistance level (Wang et al. 2020). Similar to our findings, the pore structure of *R. japonicum* leaves was moderately damaged by formaldehyde stress.

4.2 Effect of formaldehyde stress on chlorophyll content and fluorescence of *R. japonicum*

Chloroplasts, the central organelles responsible for photosynthesis and plant regulation, play a significant role in perceiving external stimuli and adapting to environmental changes. Changes in the pigment content within chloroplasts directly affect the photosynthetic efficiency of plants. Non-biological stressors can alter the structure and content of plant chlorophyll, disrupt chlorophyll function, and affect photosynthesis. Previous studies have indicated that under formaldehyde stress, plants undergo inhibited photosynthesis and experience a reduction in chlorophyll content (Li et al. 2019, Wang et al. 2020). Our findings align with this pattern, revealing a significant decrease in chlorophyll content in *R. japonicum* following formaldehyde stress. This implies that formaldehyde affects plant chlorophyll synthesis. Chlorophyll a, a critical light-harvesting pigment, experiences reduced levels, leading to diminished light-harvesting pigment content in *R. japonicum*. This reduction affects the efficiency of light utilization, consequently affecting plant photosynthesis. Given that approximately 90% of Chl b is associated with LHCII (the light-harvesting chlorophyll a/b protein complex of PSII), the reduction in Chl b suggests the degradation of LHCII (Horie et al. 2009). Furthermore, our results indicate that the chlorophyll content in *R. japonicum* was more sensitive to formaldehyde than chlorophyll b. This may explain the significant decrease in the chlorophyll a/b ratio at moderate to high formaldehyde concentrations compared to that of the control. Our study indicates that the suppression of pigment synthesis leads to a decrease in photosynthetic activity.

Chlorophyll fluorescence serves as a classical indicator of photosynthesis, providing a nondestructive and rapid assessment of plant photosynthetic activity. Fv/Fm and Y(II) represent the theoretical and actual photosynthetic efficiencies of Photosystem II (PSII), respectively, both serving as indicators of photosynthesis efficiency. As formaldehyde concentrations increased, both Fv/Fm and Y(II) decreased, highlighting a significant influence of formaldehyde on the photosynthetic efficiency of *R. japonicum* PSII and a reduction in overall its photosynthetic activity. Photochemical quenching (qP) indicates plant photosynthetic activity. In contrast, non-photochemical quenching (qN) reflects the ability of the plant to dissipate excess light energy as heat, serving as a measure of photoprotective capacity. As formaldehyde concentration increased, qP decreased, and qN increased. This indicates that under moderate to high formaldehyde stress, the photosynthetic activity of *R. japonicum* is inhibited, prompting the plant to activate photoprotective mechanisms for dissipating excess light energy and protecting the photosynthetic apparatus(Ren et al. 2022). In conclusion, formaldehyde stress affected chlorophyll

synthesis and disrupted photosynthesis in *R. japonicum*. Moreover, *R. japonicum* may respond to stress by increasing thermal dissipation.

4.3 Effect of formaldehyde stress on the fast-phase fluorescence of chlorophyll in *R. japonicum*

Chlorophyll OJIP fluorescence kinetics analysis, a non-destructive detection method widely utilized for assessing the influence of non-biological stress on plant photosynthetic metabolism(Goltsev et al. 2016), was used to assess the effects of formaldehyde stress on photosystem II in *R. japonicum*. A more detailed understanding of the damage to photosystem II was achieved through chlorophyll fast fluorescence. In this analysis, point O represents the initial fluorescence, and its intensity correlates with the content of the antenna pigments and the activity of the reaction center. The initial fluorescence decreased with increasing formaldehyde concentration, possibly because of the decrease in chlorophyll content in *R. japonicum* compared to the control group. Point P represents the maximum fluorescence, and its magnitude is related to the structure and function of the antenna and the extent of energy dissipation. As formaldehyde concentration increased, the maximum fluorescence decreased compared to the control group, possibly because of damage to the photosynthetic antenna. Through double normalization of the OJIP curve and individual stage analyses, the emergence of L and K peaks was identified after formaldehyde treatment. Compared to the control group, the appearance of the L peak was observed in the formaldehyde treatment group, while the highest L peak was observed in the high-concentration group. These findings indicate that the presence of formaldehyde led to antenna pigment complex dissociation. This results in further *R. japonicum* thylakoid membrane integrity damage (Fig. 3C). The K step length (300μs) in the chlorophyll fluorescence transient serves as an indicator of damage to the oxygen-evolving complex (OEC) in the photosynthetic apparatus. The K step length in the treatment group was significantly higher than in the control group (Fig. 3D), indicating the inhibition of donor-side PSII activity and damage to the OEC. The peaks of the L and K signals were most prominent at high formaldehyde concentrations, indicating the degradation of the photosynthetic apparatus in *R. japonicum* under formaldehyde stress, with more severe damage observed at higher concentrations.

4.4 Effect of formaldehyde stress on the rapid light response curve of *R. japonicum*

The Dual-PAM-100 system, offering simultaneous measurements of chlorophyll fluorescence and P700 + absorbance, provides a valuable tool for assessing changes in both PSII and PSI. This system proves accurate, rapid, and effective for toxicological bioassays. Data obtained from the Dual-PAM-100 system are used to analyze the activities of PSI and PSII under formaldehyde treatment. As formaldehyde concentrations increased, Y(I), Y(II), ETR(I), and ETR(II) showed decreasing trends, whereas Y(ND) and Y(NO) showed increasing trends. The increase in Y(NO) indicates an elevated proportion of closed PSII centers and the inability of reaction centers to cope with excessive light under high levels of formaldehyde stress. Formaldehyde stress reduced the quantum yields of PSI and PSII and the relative linear electron flow rate while imposing constraints on the donor side of PSI. The significant increase in

Y(ND) and the relatively modest alteration in Y(NA) indicate that the decrease in the quantum yield of PSI was mainly owing to limitations on the donor side of PSI. Y(ND) represents the fraction of P700 oxidized because of the deficiency of donors or electron deprivation in PSI. The small antenna size in PSII effectively limits the photochemistry of PSI by inefficiently absorbing light and encountering donor-side limitations(Huang et al. 2010). The significant Y(ND) increase under formaldehyde stress indicated that PSI remains well-regulated even after formaldehyde treatment. This decrease in PSI photochemistry was owing to insufficient electron donors and light absorption by PSI.(Deng et al. 2013). PSI plays a vital role in cyclic electron flow, generating a trans-thylakoid proton gradient (ΔpH) for ATP synthesis. A decrease in Y(I) indicates significant impairment of photosynthetic function(Bailey et al. 2008). The concurrent reduction in Y(I) and Y(II) indicated that formaldehyde stress inhibited electron transfer in both PSII and PSI of moss. The decrease in ETRmax(II) and ETRmax(I) (Table 2) and increase in Y(ND) (Fig. 4B) confirmed this inhibitory effect.

As the formaldehyde concentration increased, a significant rise in the rate of CEF was observed compared to that of the control, indicating the activation of CEF under formaldehyde stress. CEF around PSI mitigates damage from excess electron flow to PSI by generating ΔpH(Ren et al. 2022). ΔpH plays an important role in regulating photosynthesis by modulating the light-harvesting efficiency of antennae through the qE mechanism, facilitating the dissipation of excess light energy. The generation of ΔpH also slows down the electron transfer from PSII to PSI through Cytb6f, preventing over-reduction of the PSI reaction center and reducing the production of superoxide and singlet oxygen in the thylakoid membrane(Takagi et al. 2017). ΔpH serves as a central signal, stabilizing the oxygen-evolving complex and activating NPQ(Tan et al. 2020, Tikkanen &Aro 2014). Activation of CEF and NPQ is an important mechanism for protecting the photosynthetic apparatus under formaldehyde stress. The proton gradient activates NPQ, and an increase in NPQ leads to the harmless dissipation of excess excitation energy as heat, demonstrating the protective function of the photosynthetic apparatus. Various abiotic stresses, including high temperature, high light, and low temperature, can reduce the ability of plants to absorb and utilize light, resulting in the accumulation of excess light energy in the photosystem, thereby influencing photosystem activity and reducing photosynthetic efficiency(Faik et al. 2016, Zhou et al. 2018). To prevent excessive damage to photosystems, plants may dissipate the excess energy accumulated in PSII and PSI centers through mechanisms such as NPQ, the xanthophyll cycle, state transitions, and alternative electron pathways(Lu et al. 2020, Pinnola &Bassi 2018).

4.5 Effects of formaldehyde stress on the antioxidant physiology of *R. japonicum*

In stressful conditions, a reduction in the light utilization efficiency leads to an increase in excess excitation energy, resulting in the generation of ROS. When the light intensity suddenly increased, the electron transfer from PSII to PSI increased rapidly, but the CO2 fixation occurred more slowly. Consequently, the products of linear electron transfer, ATP and NADPH, cannot be immediately utilized by the Calvin cycle. This leads to the accumulation of reduced power within PSI(Chovancek et al. 2019, Lu et al. 2017). If alternative electron flows do not quench excess electrons in PSI, ROS are generated in PSI,

causing damage. ROS comprises a group of oxygen-derived single-electron reduction products with high redox potentials, including singlet oxygen (^1O), superoxide anion ($O_2^{\cdot-}$), hydroxyl radical (·OH), and hydrogen peroxide (H_2O_2), among others. ROS are prevalent throughout plants, and endogenous ROS primarily stem from non-photosynthetic pathways in mitochondria and peroxisomes and photosynthetic metabolism in chloroplasts. ROS generation occurs during chloroplast water electrolysis, electron transfer, and photosynthetic phosphorylation. The photosynthetic pathway in plants is particularly sensitive to stress and serves as a major source of ROS.(Takagi et al. 2017). ROS, serving as important signaling molecules, are widely present in plants. Plants maintain a dynamic balance between ROS production and clearance by regulating enzyme-mediated antioxidant systems and synthesizing non-enzymatic antioxidants(Bobrovskikh et al. 2020, Zhanassova et al. 2021). The plant antioxidant enzyme system includes various enzymes, such as SOD, CAT, and POD, constituting vital pathways for plants to resist oxidative stress. Non-enzymatic antioxidants, such as ascorbic acid (ASA) and reduced glutathione (GSH), play a crucial role in plants. They directly scavenge ROS and are extensively involved in plant oxidative stress responses. Formaldehyde induces the production of superoxide anions in *R. japonicum*, typically originating from chloroplast photosystems I and II. This suggests that under formaldehyde stress, the amount of light quantum absorbed by photosynthetic pigments exceeds the energy required for *R. japonicum* to fix CO_2, potentially leading to the production of superoxide anions in chloroplasts owing to excess light energy. Within plant cells, superoxide anions have a short lifespan. They can be converted to hydrogen peroxide by SOD catalysis, which is then decomposed into water and oxygen by POD and CAT catalysis, respectively. Increased SOD activity promotes the conversion of superoxide anions into hydrogen peroxide, whereas increased POD and CAT activities facilitate the conversion of hydrogen peroxide into water, thereby preventing the accumulation of excessive hydrogen peroxide and cellular oxidative damage. The findings indicate that *R. japonicum* can experience disturbances in intracellular ROS levels at low to moderate formaldehyde concentrations. However, the responsive action of intracellular antioxidant enzymes effectively prevents oxidative damage caused by ROS accumulation. This mechanism shows how *R. japonicum* copes with formaldehyde-induced stress. MDA serves as a reliable indicator of membrane damage resulting from oxidative stress, particularly due to membrane lipid peroxidation(Peng et al. 2022). When *R. japonicum* faces low-to-moderate concentrations of formaldehyde, activating the antioxidant enzyme system eliminates ROS within cells effectively. The generation and clearance of ROS reach a dynamic balance, thereby protecting cells. However, at high formaldehyde concentrations, the activities of the three enzymes in the antioxidant system significantly decreased. ROS (hydrogen peroxide and superoxide anions) accumulate within cells without proper clearance, leading to membrane lipid peroxidation and increased MDA content.

5. Conclusions

This study investigated the toxic effects of formaldehyde on *R. japonicum*, specifically focusing on its structural integrity, photosynthetic pigment levels, and the functionality of PSI, PSII, and antioxidant systems. To understand the effects of formaldehyde exposure comprehensively, we examined changes in the quantum yield of PSI, PSII, and CEF, along with alterations in the electron transfer rates of PSI and

PSII from a photosynthetic standpoint. The generation and elimination of ROS were analyzed from an antioxidant physiology perspective. From both the photosynthetic and antioxidant physiological perspectives, the response mechanisms of *R. japonicum* under different concentrations of formaldehyde stress were systematically elucidated. *R. japonicum* responded to moderate to low formaldehyde concentrations by engaging its antioxidant system to eliminate ROS interference. Contrastingly, under high formaldehyde concentrations, the activity of the antioxidant enzyme system in *R. japonicum* decreased. In contrast, CEF was activated to protect PSI from excessive reduction and damage to the photosynthetic apparatus. Simultaneously, NPQ is activated to dissipate excess light energy through thermal dissipation. This study systematically explored the response mechanisms of plants to formaldehyde stress, offering insights for future monitoring of formaldehyde and other indoor toxic gases.

Abbreviations

ROS: reactive oxygen species; SEM: scanning electron microscope; FW: fresh weight; MDA: malondialdehyde; DAB: 3,3-diaminobenzidine; NBT: nitroblue tetrazolium; SOD: superoxide dismutase; POD: peroxidase; CAT: catalase; APX: ascorbate peroxidase; DHAR: dehydroascorbate reductase; MDHAR: monodehydroascorbate reductase; qP: photochemical quenching; qN: non-photochemical quenching; PS: photosystem; ASA: ascorbic acid; GSH: reduced glutathione

Declarations

Ethical Approval : This article does not contain any studies with human participants or animals performed by any of the authors

Consent to Participate Not applicable

Consent to Publication: All authors have read and approved this manuscript to be considered for publication.

Author contributions: Wanting Li, Yunmei Lu and Ke Chen conceived and designed research. Wanting Li, Siqi Ma, Haiyan Qiu, Xiaoping Yang and Hao Tang conducted experiments. Wanting Li, Peng Ren, Renhua Huang and Yunlai Tang analyzed data. Wanting Li, Siqi Ma, Qunlong Chen and Ke Chen wrote the draft of the manuscript and intensively edited by all authors. All authors have read and agreed to the published version of the manuscript.

Funding: This research was funded by Sichuan province transfer payment application project (R22ZYZF0001); Jingmen key science and technology plan projects (2023YFZD014); Innovation and entrepreneurship project of college student in Sichuan Province (S202310619050).

Competing interests: The authors declare no conflict of interest.

References

1. Achary VMM, Jena S, Panda KK, Panda BB (2008) Aluminium induced oxidative stress and DNA damage in root cells of *Allium cepa L*. Ecotoxicol Environ Saf 70:300–310
2. Adam MG, Tran PTM, Bolan N, Balasubramanian R (2021) Biomass burning-derived airborne particulate matter in Southeast Asia: A critical review. J Hazard Mater 407:124760
3. Anonymous List of (2020) Classifications – IARC Monographs on the Identification of Carcinogenic Hazards to Humans. Monogr iarc who int
4. Bailey S, Melis A, Mackey KRM, Cardol P, Finazzi G, van Dijken G, Berg GM, Arrigo K, Shrager J, Grossman A (2008) Alternative photosynthetic electron flow to oxygen in *marine Synechococcus*. Biochim et Biophys Acta (BBA) - Bioenergetics 1777:269–276
5. Bargagli R (2016) Moss and lichen biomonitoring of atmospheric mercury: A review. Sci Total Environ 572:216–231
6. Bobrovskikh A, Zubairova U, Kolodkin A, Doroshkov A (2020) : Subcellular compartmentalization of the plant antioxidant system: an integrated overview. PeerJ 8
7. Burgos-Barragan G, Wit N, Meiser J, Dingler FA, Pietzke M, Mulderrig L, Pontel LB, Rosado IV, Brewer TF, Cordell RL, Monks PS, Chang CJ, Vazquez A, Patel KJ (2017) Mammals divert endogenous genotoxic formaldehyde into one-carbon metabolism. Nature 548:549–554
8. Chaligava O, Shetekauri S, Badawy WM, Frontasyeva MV, Zinicovscaia I, Shetekauri T, Kvlividze A, Vergel K, Yushin N (2021) Characterization of Trace Elements in Atmospheric Deposition Studied by Moss Biomonitoring in Georgia. Arch Environ Contam Toxicol 80:350–367
9. Chovancek E, Zivcak M, Botyanszka L, Hauptvogel P, Yang X, Misheva S, Hussain S, Brestic M (2019) Transient heat waves may affect the photosynthetic capacity of susceptible wheat genotypes due to insufficient photosystem I photoprotection. Plants 8:282
10. Deng C, Zhang D, Pan X, Chang F, Wang S (2013) Toxic effects of mercury on PSI and PSII activities, membrane potential and transthylakoid proton gradient in *Microsorium pteropus*. J Photochem Photobiol B 127:1–7
11. Faik A, Popova A, Velitchkova M (2016) Effects of long-term action of high temperature and high light on the activity and energy interaction of both photosystems in tomato plants. Photosynthetica 54:611–619
12. Gallego-Cartagena E, Morillas H, Carrero JA, Madariaga JM, Maguregui M (2021) Naturally growing grimmiaceae family mosses as passive biomonitors of heavy metals pollution in urban-industrial atmospheres from the Bilbao Metropolitan area. Chemosphere 263:128190
13. Goltsev VN, Kalaji HM, Paunov M, Bąba W, Horaczek T, Mojski J, Kociel H, Allakhverdiev SI (2016) Variable chlorophyll fluorescence and its use for assessing physiological condition of plant photosynthetic apparatus. Russ J Plant Physiol 63:869–893

14. Hodgson AT, Beal D, McIlvaine JER (2002) Sources of formaldehyde, other aldehydes and terpenes in a new manufactured house. Indoor Air 12:235–242
15. Horie Y, Ito H, Kusaba M, Tanaka R, Tanaka A (2009) Participation of chlorophyll b reductase in the initial step of the degradation of light-harvesting chlorophyll a/b-protein complexes in *Arabidopsis*. J Biol Chem 284:17449–17456
16. Huang W, Zhang SB, Cao KF (2010) Stimulation of Cyclic Electron Flow During Recovery After Chilling-Induced Photoinhibition of PSII. Plant Cell Physiol 51:1922–1928
17. Kim KJ, Jeong MI, Lee DW, Song JS, Kim HD, Yoo EH, Jeong SJ, Han SW, Kays SJ, Lim Y-W, Kim H-H (2010) Variation in Formaldehyde Removal Efficiency among Indoor Plant Species. HortScience horts 45:1489–1495
18. Krommer V, Zechmeister HG, Roder I, Scharf S, Hanus-Illnar A (2007) Monitoring atmospheric pollutants in the biosphere reserve Wienerwald by a combined approach of biomonitoring methods and technical measurements. Chemosphere 67:1956–1966
19. Kwon K-J, Kwon H-J, Oh Y-A, Kim S-Y, Park B-J (2021) : Particulate Matter Removal of Three Woody Plant Species, *Ardisia crenata*, *Ardisia japonica*, and *Maesa japonica*. Sustainability 13, 11017
20. Li J, Zhong J, Zhan T, Liu Q, Yan L, Lu M (2019) Indoor formaldehyde removal by three species of *Chlorphytum Comosum* under the long-term dynamic fumigation system. Environ Sci Pollut Res Int 26:36857–36868
21. Li WT, Chen K, Li Q, Tang YL, Jiang YY, Su Y (2023) : Effects of Arbuscular Mycorrhizal Fungi on Alleviating Cadmium Stress in *Medicago truncatula Gaertn*. Plants-Basel 12
22. Liang H, Zhao S, Su Y (2018) Self-Enhancement Effect and Mechanism of Potted Chlorophytum comosum on Formaldehyde Removal from Air. Int J Environ Res 12:337–346
23. Lu J, Yin Z, Lu T, Yang X, Wang F, Qi M, Li T, Liu Y (2020) : Cyclic electron flow modulate the linear electron flow and reactive oxygen species in tomato leaves under high temperature. Plant Sci 292
24. Lu T, Meng Z, Zhang G, Qi M, Sun Z, Liu Y, Li T (2017) Sub-high temperature and high light intensity induced irreversible inhibition on photosynthesis system of tomato plant (*Solanum lycopersicum L.*). Front. Plant Sci 8:365
25. Mahapatra B, Dhal NK, Dash AK, Panda BP, Panigrahi KCS, Pradhan A (2019) Perspective of mitigating atmospheric heavy metal pollution: using mosses as biomonitoring and indicator organism. Environ Sci Pollut Res 26:29620–29638
26. McGregor D, Bolt H, Cogliano V, Richter-Reichhelm H-B (2006) Formaldehyde and Glutaraldehyde and Nasal Cytotoxicity: Case Study Within the Context of the 2006 IPCS Human Framework for the Analysis of a Cancer Mode of Action for Humans. Crit Rev Toxicol 36:821–835
27. Peng WX, Yue X, Chen H, Ma NL, Quan Z, Yu Q, Wei Z, Guan R, Lam SS, Rinklebe J, Zhang D, Zhang B, Bolan N, Kirkham MB, Sonne C (2022) A review of plants formaldehyde metabolism: Implications for hazardous emissions and phytoremediation. J Hazard Mater 436:129304
28. Pinnola A, Bassi R (2018) Molecular mechanisms involved in plant photoprotection. Biochem Soc Trans 46:467–482

29. Rao MV, Davis KR (1999) Ozone-induced cell death occurs via two distinct mechanisms in *Arabidopsis*: the role of salicylic acid. Plant J 17:603–614
30. Ren H, Huang R, Li Y, Li W, Zheng L, Lei Y, Chen K (2022) Photosynthetic regulation in response to strontium stress in moss *Racomitrium japonicum L*. Environ Sci Pollut Res 30:20923–20933
31. Salonen H, Pasanen AL, Lappalainen S, Riuttala H, Tuomi T, Pasanen P, Bäck B, Reijula K (2009) Volatile Organic Compounds and Formaldehyde as Explaining Factors for Sensory Irritation in Office Environments. J Occup Env Hyg 6:239–247
32. Sheng X, Zhaohui Z, Zhihui W (2022) : Potentially toxic elements have adverse effects on moss communities in the manganese mines of Southern China. Environ Pollut 305
33. Srivastava S, Brychkova G, Yarmolinsky D, Soltabayeva A, Samani T, Sagi M (2017) Aldehyde oxidase 4 plays a critical role in delaying silique senescence by catalyzing aldehyde detoxification. Plant Physiol 173:1977–1997
34. Stafilov T, Sajn R, Barandovski L, Andonovska KB, Malinovska S (2018) Moss biomonitoring of atmospheric deposition study of minor and trace elements in Macedonia. Air Qual Atmos Health 11:137–152
35. Świsłowski P, Hrabák P, Wacławek S, Liskova K, Antos V, Rajfur M, Ząbkowska-Wacławek M (2021) : The Application of Active Biomonitoring with the Use of Mosses to Identify Polycyclic Aromatic Hydrocarbons in an Atmospheric Aerosol. Molecules 26
36. Takagi D, Amako K, Hashiguchi M, Fukaki H, Ishizaki K, Goh T, Fukao Y, Sano R, Kurata T, Demura T, Sawa S, Miyake C (2017) Chloroplastic ATP synthase builds up a proton motive force preventing production of reactive oxygen species in photosystem I. Plant J 91:306–324
37. Tan S-L, Yang Y-J, Liu T, Zhang S-B, Huang W (2020) : Responses of photosystem I compared with photosystem II to combination of heat stress and fluctuating light in tobacco leaves. Plant Sci 292
38. Tang X, An B, Cao D, Xu R, Wang S, Zhang Z, Liu X, Sun X (2020) : Improving Photosynthetic Capacity, Alleviating Photosynthetic Inhibition and Oxidative Stress Under Low Temperature Stress With Exogenous Hydrogen Sulfide in Blueberry Seedlings. Front. Plant Sci. 11
39. Tikkanen M, Aro E-M (2014) Integrative regulatory network of plant thylakoid energy transduction. Trends Plant Sci 19:10–17
40. Vash IY (2020) The influence of in utero exposure to formaldehyde on newborn rat thymus structure. RMBH 28:143–152
41. Wang L, Sheng Q, Zhang Y, Xu J, Zhang H, Zhu Z (2020) Tolerance of fifteen hydroponic ornamental plant species to formaldehyde stress. Environ Pollut 265:115003
42. Wolverton B (1985) : Foliage plants for removing air pollutants from energy-efficient buildings
43. Xia H, Chen K, Liu L, Plenkovic-Moraj A, Sun G, Lei Y (2022) : Photosynthetic regulation in fluctuating light under combined stresses of high temperature and dehydration in three contrasting mosses. Plant Sci 323

44. Xu Z, Wang L, Hou H (2011) Formaldehyde removal by potted plant-soil systems. J Hazard Mater 192:314–318
45. Yergaliyev TM, Nurbekova Z, Mukiyanova G, Akbassova A, Sutula M, Zhangazin S, Bari A, Tleukulova Z, Shamekova M, Masalimov ZK (2016) The involvement of ROS producing aldehyde oxidase in plant response to *Tombusvirus* infection. Plant Physiol Biochem 109:36–44
46. Yesbergenova Z, Yang G, Oron E, Soffer D, Fluhr R, Sagi M (2005) The plant Mo-hydroxylases aldehyde oxidase and xanthine dehydrogenase have distinct reactive oxygen species signatures and are induced by drought and abscisic acid. Plant J 42:862–876
47. Zhanassova K, Kurmanbayeva A, Gadilgereyeva B, Yermukhambetova R, Iksat N, Amanbayeva U, Bekturova A, Tleukulova Z, Omarov R, Masalimov Z (2021) : ROS status and antioxidant enzyme activities in response to combined temperature and drought stresses in barley. Acta Physiol. Plant. 43
48. Zhou R, Wu Z, Wang X, Rosenqvist E, Wang Y, Zhao T, Ottosen C-O (2018) Evaluation of temperature stress tolerance in cultivated and wild tomatoes using photosynthesis and chlorophyll fluorescence. Hortic Environ Biotechnol 59:499–509

Figures

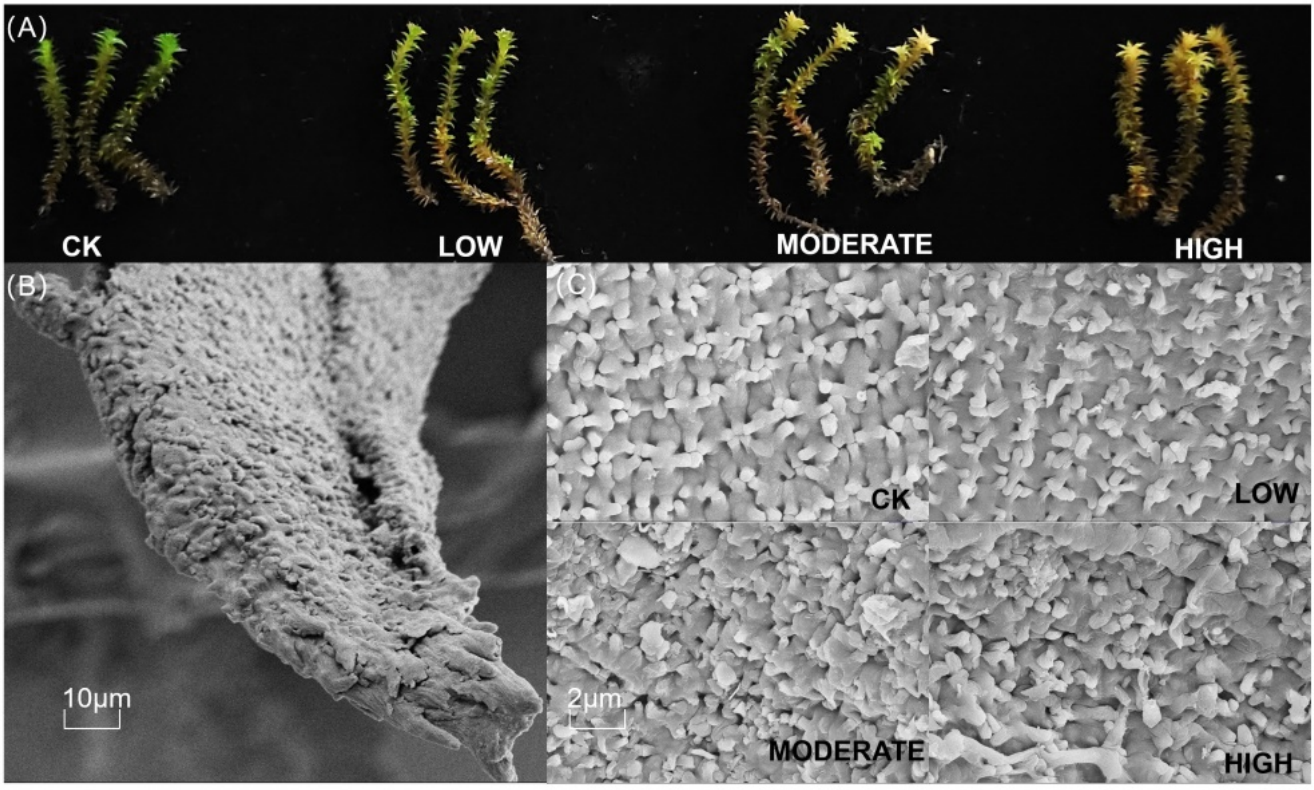


Figure 1

Morphological changes (A) and microstructural changes (C) in R. japonicum after formaldehyde stress. Fig. B presents the scanning electron microscope images of control leaves at 10 μm.

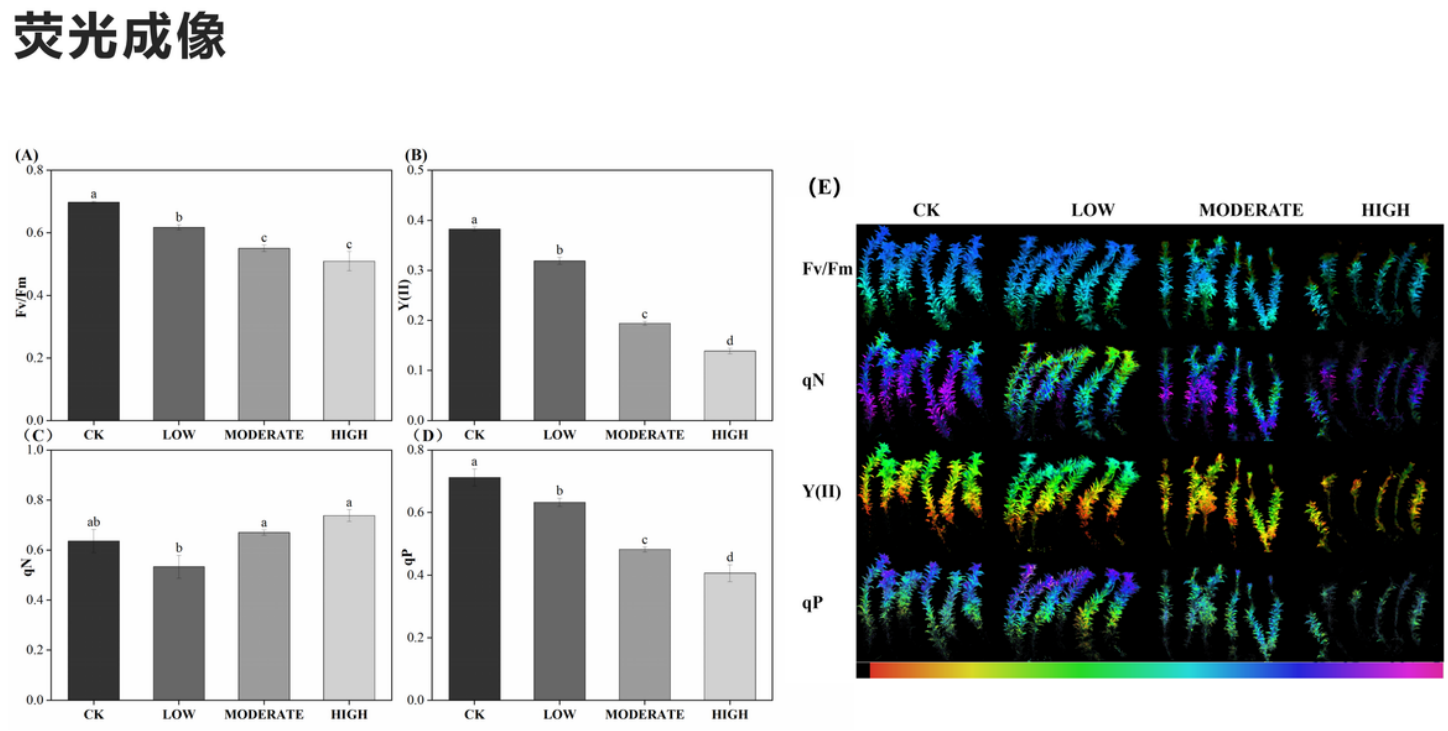


Figure 2

Chlorophyll fluorescence parameters (A, B, C, D) and imaging (E) of R. japonicum under various formaldehyde concentrations. The false color code depicted at the bottom of each image ranges from 0.000 (black) to 1.000 (pink). Values are expressed as means ± SE (n = 3). Different letters represent significant differences between treatments ($p < 0.05$).

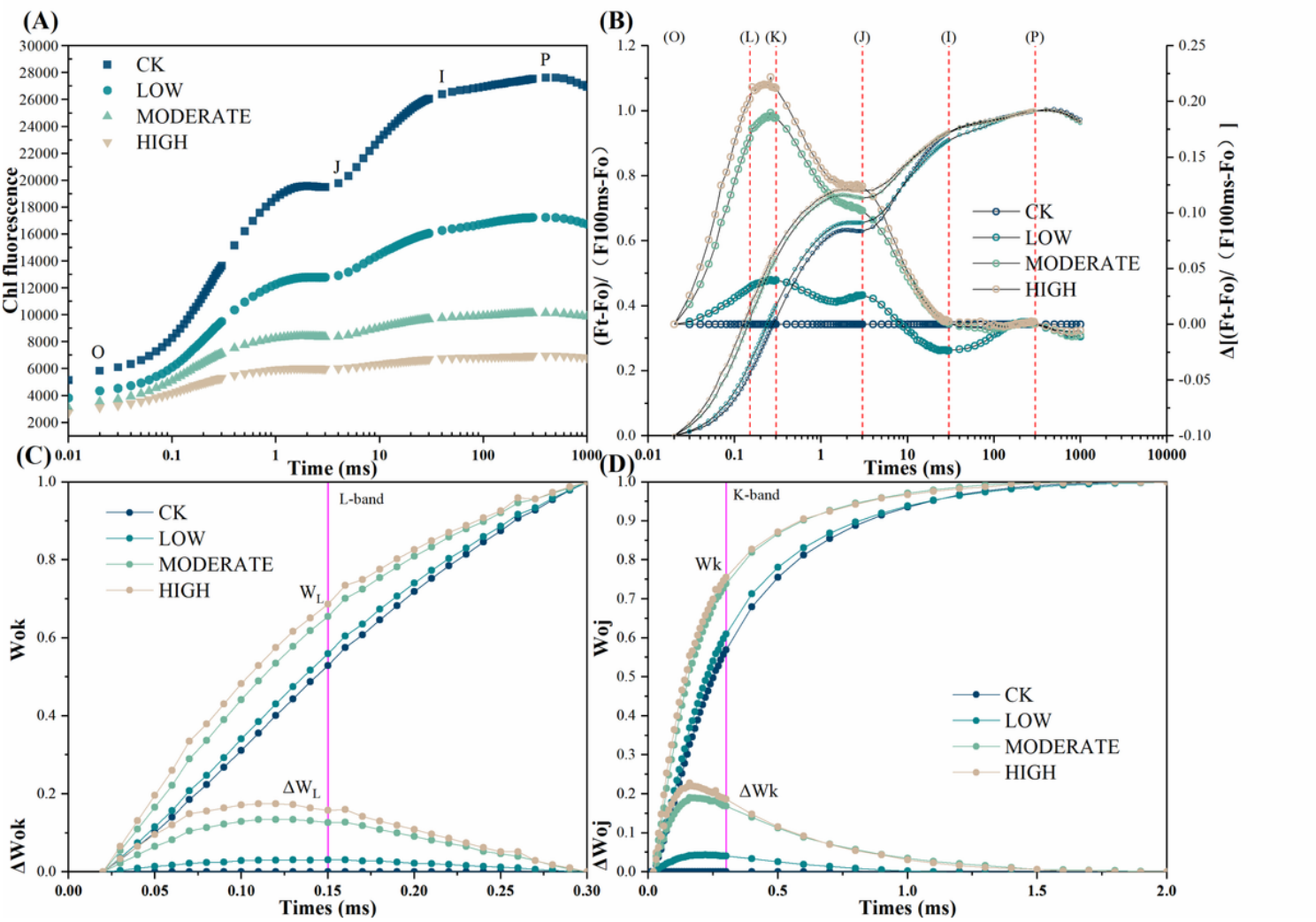


Figure 3

Chlorophyll fast-phase fluorescence of R. japonicum under varied formaldehyde concentrations. (A) Raw Chl a fluorescence rise kinetics showing different concentrations of formaldehyde stress in a logarithmic time scale. (B) Chl a fluorescence rise kinetics normalized by FO and FM as Vt = (Ft -FO)/(FM-FO) in a logarithmic time scale. ΔVt = Vt(treatment)-Vt(control). (C) The fluorescence rise kinetics normalized by FO and FK as WOK = (Ft − FO)/(FK − FO), and the difference kinetics ΔWOK = WOK(treatment) − WOK (control) in a linear time scale from 0 to 300 μs. (D) Fluorescence rise kinetics normalized by FO and FJ as WOJ = (Ft − FO)/(FJ − FO) , and the difference kinetics ΔWOJ = WOJ(treatment) − WOJ(control) in a linear time scale from 0 to 2 ms.

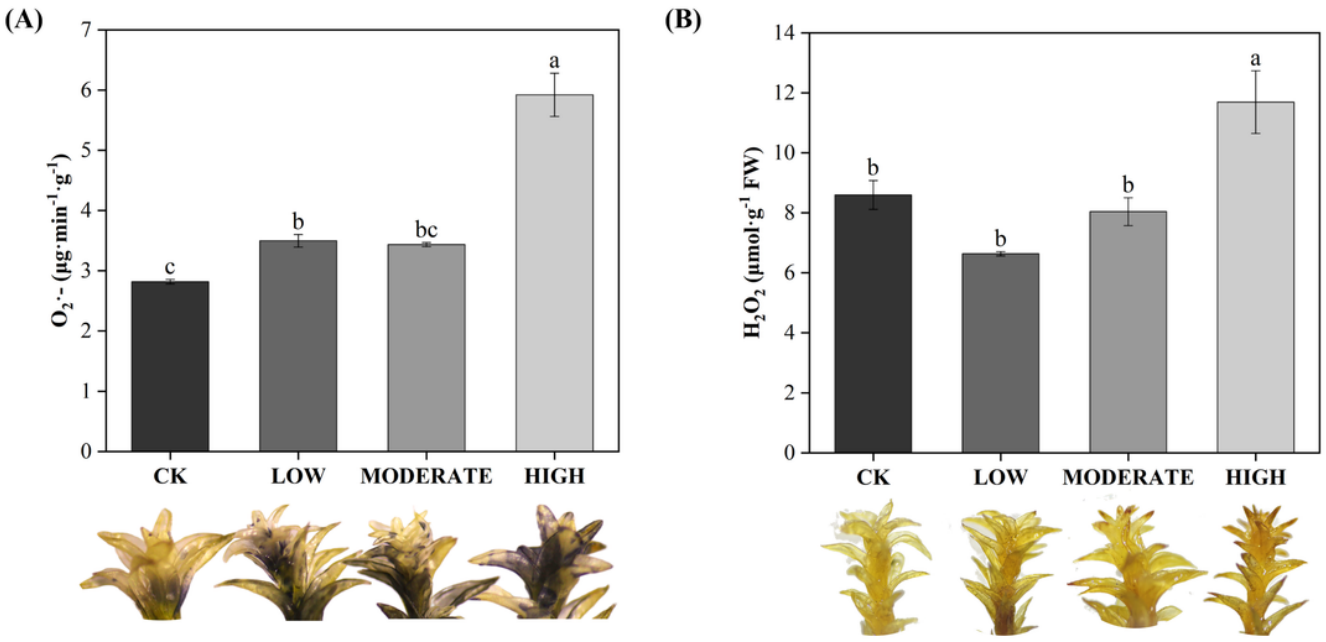


Figure 4

Rapid light response curve of R. japonicum under varied formaldehyde stress concentrations. (A) Y(I), (B) Y(ND), (C) Y(NA), (D) Y(II), (E) Y(NO), (F) Y(NPQ), (G) ETRI, (H) ETRII, (I) ETRI-ETRII.

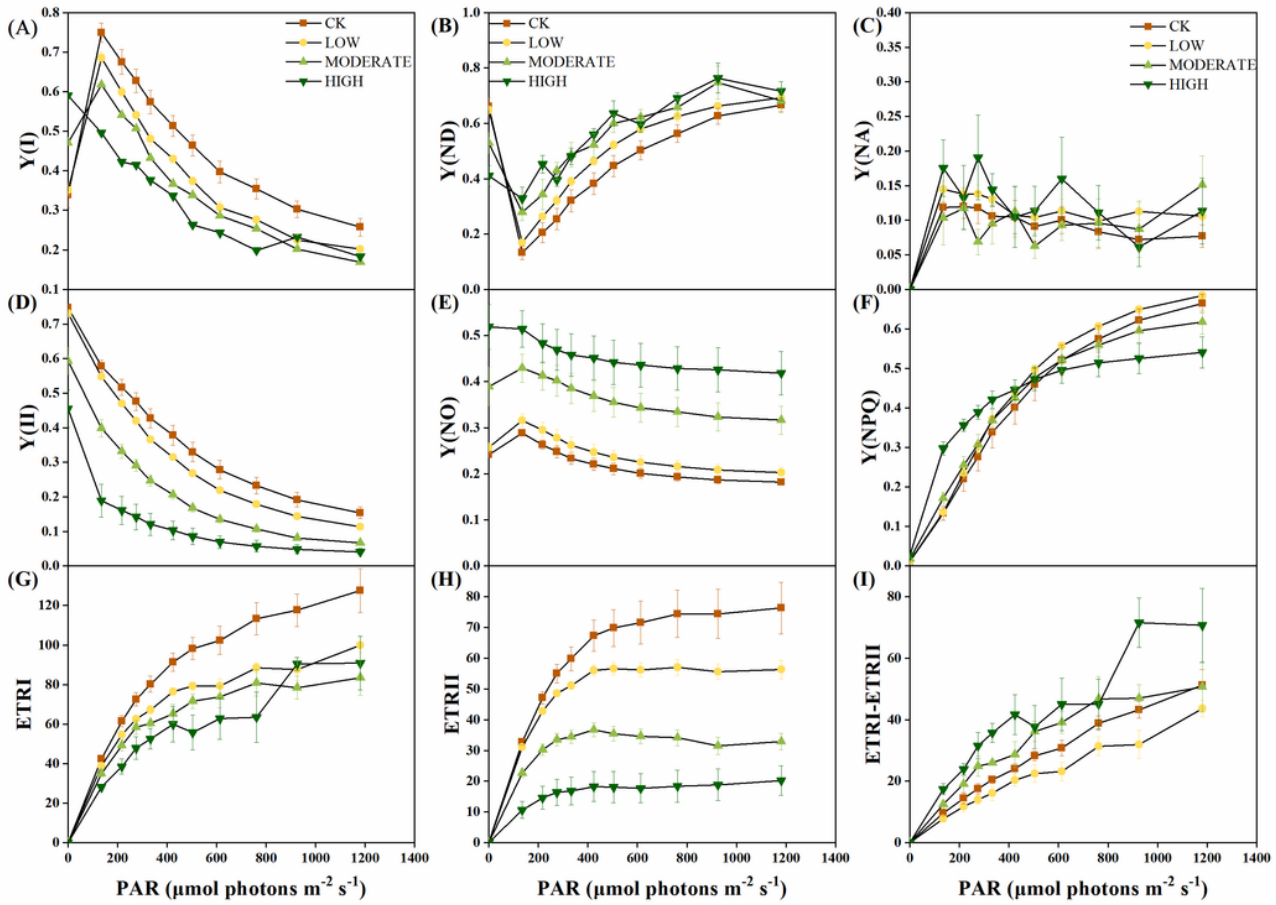


Figure 5

Effects of different concentrations of formaldehyde stress on the content of reactive oxygen species in R. japonicum. (A) Superoxide anion content and leaf staining in R. japonicum. (B) hydrogen peroxide content and leaf staining in R. japonicum. Values are expressed as means ± SE (n = 3). Different letters represent significant differences between treatments ($p < 0.05$).

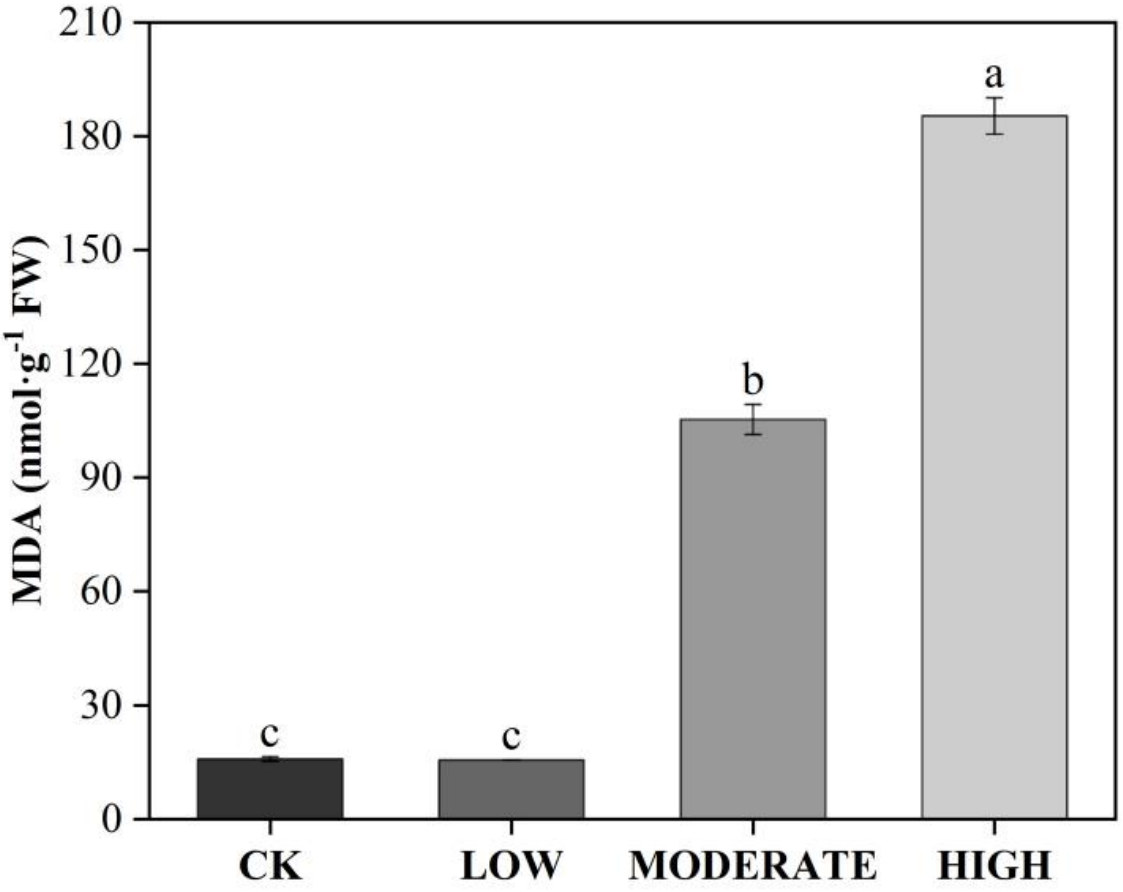


Figure 6

Effects of different concentrations of formaldehyde stress on the MDA content of R. japonicums. Values are expressed as means ± SE (n = 3). Different letters represent significant differences between treatments ($p < 0.05$).

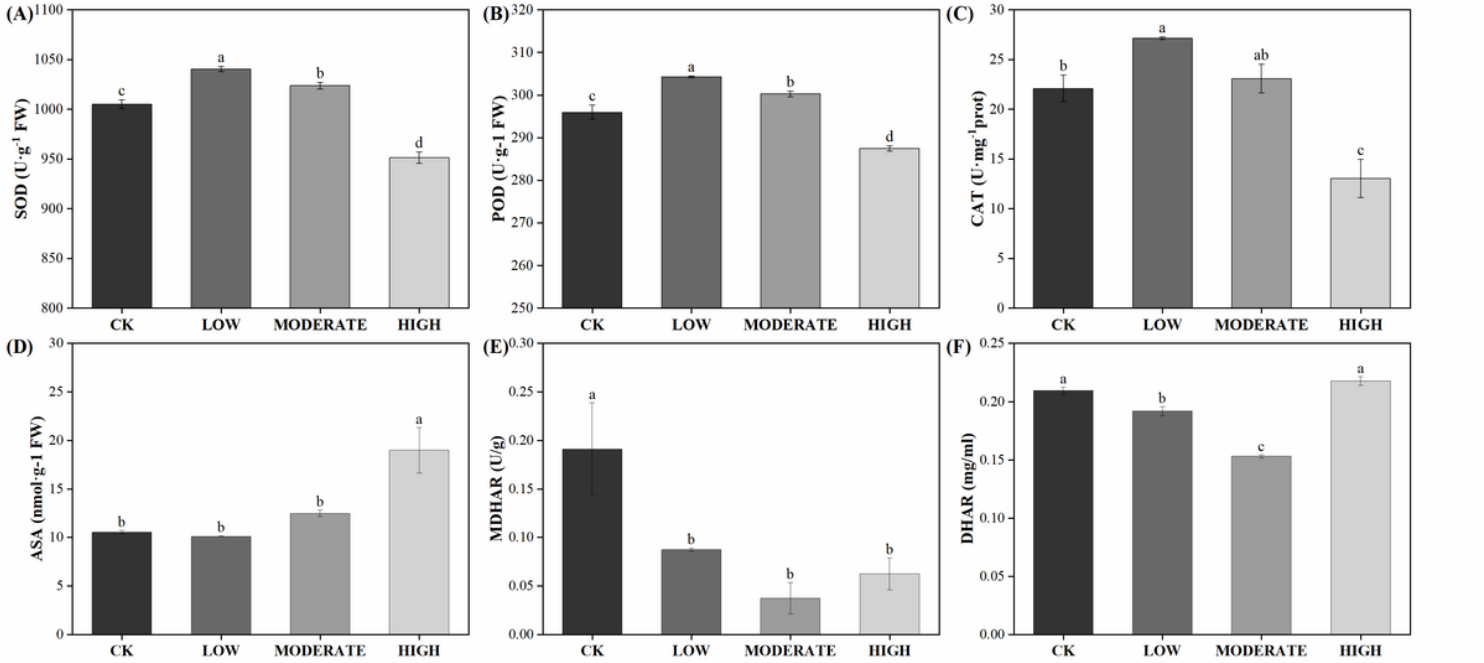


Figure 7

Effects of varied concentrations of formaldehyde stress on the antioxidant system) of R. japonicum. (A) SOD, (B) POD, (C) CAT, (D) ASA, (E) MDHAR, (F) DHAR. Values are expressed as means ±SE (n = 3).

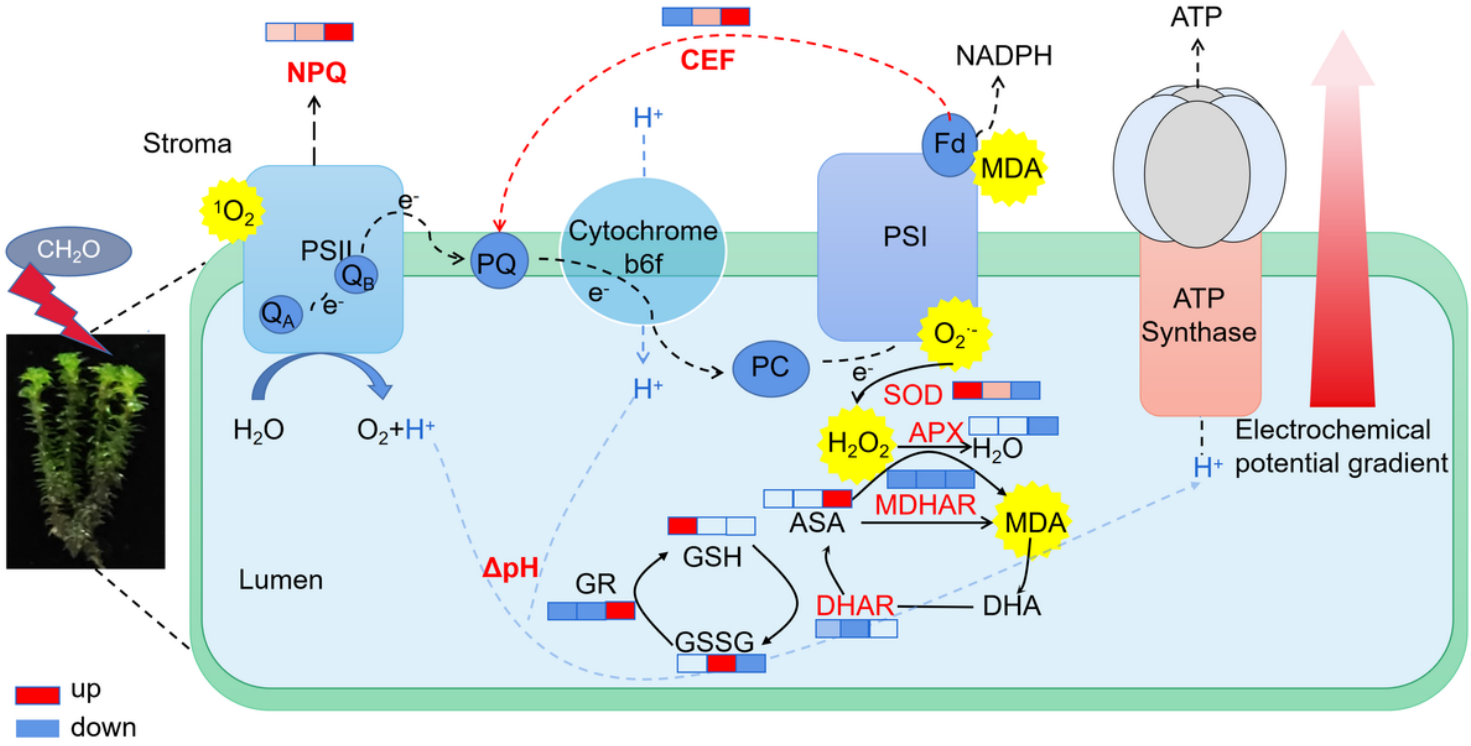


Figure 8

Electron transport and antioxidant physiological changes in R. japonicum under various formaldehyde concentrations. The boxes in the figure, from left to right, represent the low, moderate, and high concentration groups. The colors in the boxes indicate changes compared to the control group, with red representing up-regulation and blue representing down-regulation; the shade of the color indicates the degree of change.